Acta Crystallographica Section C
Crystal Structure Communications
ISSN 0108-2701

Two forms of aluminium phosphate tridymite from X-ray powder data

Heribert Graetsch

Institut für Mineralogie, Ruhr-Universität Bochum, D-44780 Bochum, Germany
Correspondence e-mail: heribert.graetsch@ruhr-uni-bochum.de

Received 13 September 1999
Accepted 23 November 1999

Monoclinic and triclinic (pseudo-orthorhombic) $AlPO_4$ tridymites have been refined from X-ray powder diffraction data using the silica analogues as starting models. The framework structures of both forms of tridymite are made up of six-membered rings of tetrahedra which differ in the distortion patterns of the ring shapes. Ordered occupation of alternate tetrahedra by Al and P leads to a doubling of the *a* lattice parameter for monoclinic $AlPO_4$ tridymite (space group *Pc*) and loss of the C-centring with respect to the isotypic silica tridymite (space group *Cc*). Triclinic $AlPO_4$ tridymite was refined in the same space group (*F*1) as the SiO_2 analogue.

Comment

$AlPO_4$ exhibits modifications with quartz, cristobalite and tridymite-type crystal structures like SiO_2. The high-temperature forms cristobalite and tridymite persist metastably at ambient conditions. All three modifications undergo displacive phase transitions at elevated temperatures. Tridymite shows a sequence of transitions from the hexagonal high-temperature form through a pseudo-orthorhombic and an incommensurate monoclinic intermediate phase to monoclinic and triclinic (pseudo-orthorhombic) room-temperature modifications. Both low-temperature phases of $AlPO_4$ tridymite co-exist and are often intergrown in the same crystal which additionally shows multiple transformation twinning (Löns *et al.*, 1989). The monoclinic form can be transformed into the triclinic modification by mechanical stress, *e.g.* by grinding. This transformation can be partially reversed by reheating (Spiegel *et al.*, 1990). In the case of SiO_2, mechanically or thermally introduced stress leads to the transformation of monoclinic tridymite to another monoclinic phase which has an incommensurate displacive modulation. This phase has not been found for $AlPO_4$ (Löns *et al.*, 1989).

The present structure refinements were carried out as part of a study of the phase-transition behaviour of different forms of tridymite. The framework structure of tridymite consists of corner-sharing tetrahedra which form layers with six-membered rings of tetrahedra. Antiparallel layers are stacked in the direction of the hexagonal (or pseudo-hexagonal) *c* axis in a two-layer sequence. In the average structure of hexagonal high-temperature tridymite, the shape of the rings is hexagonal. The structure is dynamically disordered through thermal vibrations of the stiff tetrahedra. Upon cooling, several rigid unit modes (Pryde & Dove, 1998; Kihara, 1995) successively condense and form various intermediate and low-temperature phases by co-operative rotations and shifts of the tetrahedra. Viewed along the pseudo-hexagonal *c* axis, all rings of tetrahedra are distorted to oval shapes in triclinic low tridymite (space group *F*1) forming a $2 \times 2 \times 10$ superstructure with respect to hexagonal high tridymite (orthohexagonal setting). In monoclinic low tridymite, rings with oval and ditrigonal shapes occur. The ordered cation distribution leads to a doubling of the *a* axis with respect to monoclinic silica tridymite and loss of the C-centring (space groups: *Pc* for $AlPO_4$ and *Cc* for SiO_2 tridymite). The average inter-tetrahedral Al—O—P angles are 147.4° (σ = 7.8°) in

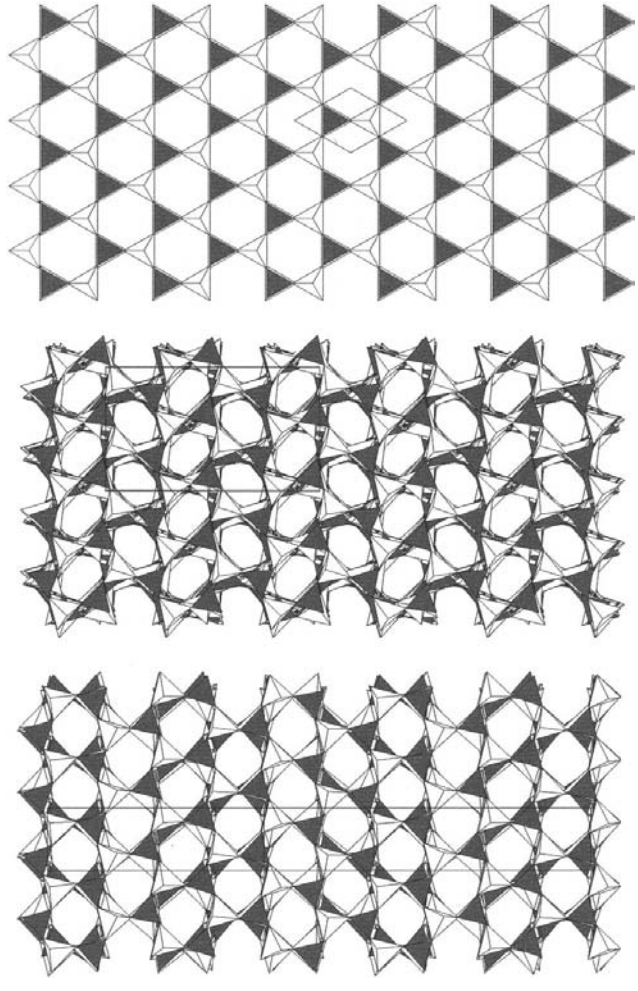

Figure 1
Polyhedral representation of hexagonal, triclinic and monoclinic $AlPO_4$ tridymites (from top to bottom). The AlO_4 tetrahedra are white and the PO_4 tetrahedra are shaded gray. The structure of hexagonal high tridymite is projected along the *c* axis, and those of triclinic and monoclinic low tridymite in a corresponding orientation are projected along their pseudo-hexagonal axes.

 © 2000 International Union of Crystallography • Printed in Great Britain – all rights reserved

triclinic and 147.6° (σ = 8.6°) in monoclinic $AlPO_4$ tridymites compared with 180° in the average structure of hexagonal high tridymite. The corresponding Si—O—Si angles are 150.0° (σ = 8.1°) in monoclinic (Baur, 1977) and 147.3° (σ = 5.0°) in triclinic silica tridymites. The calculated density of triclinic $AlPO_4$ tridymite is slightly higher (2.25 Mg m^{-3}) than that of monoclinic tridymite (2.22 Mg m^{-3}) so that the triclinic form might be considered as the more stable modification at low temperatures.

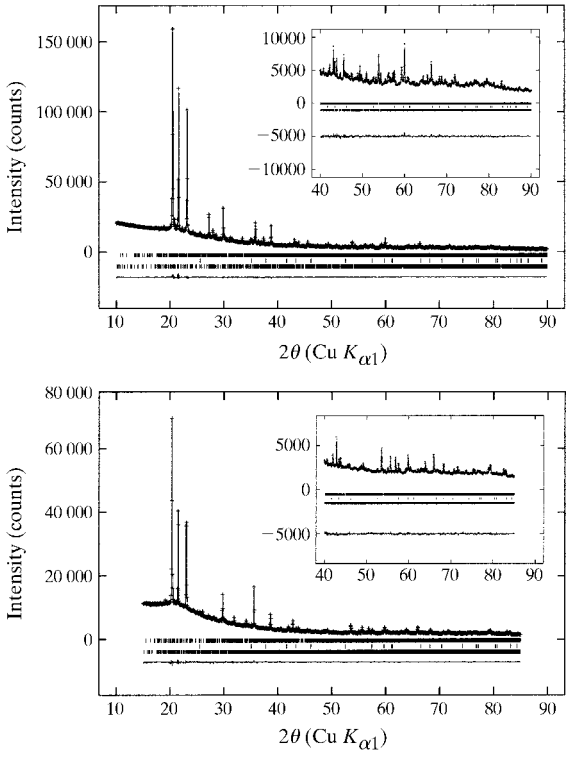

Figure 2
Comparison of observed (crosses) and calculated (solid line) intensities for triclinic (top) and monoclinic (bottom) $AlPO_4$ tridymites. The difference patterns appear below. Reflection positions are indicated by markers.

Experimental

Triclinic $AlPO_4$ tridymite was prepared by firing non-crystalline $AlPO_4$ (Merck No. 1.01098.1000) at 1273 K for one day and subsequent grinding in an agate mortar. Monoclinic $AlPO_4$ tridymite was prepared by firing at 1223 K for one day in a 0.5 mm quartz glass capillary filled with a powder of the triclinic modification. The diffractogram of this phase was recorded without previous grinding. Rietveld refinements revealed that the transformations were incomplete and both samples consisted of three phases. All samples contained 4 wt% of corundum. The sample used for the refinement of monoclinic $AlPO_4$ tridymite consisted of 88 wt% monoclinic and 8 wt% triclinic tridymite. The sample used for the refinement of triclinic tridymite consisted of 87 wt% triclinic and 9 wt% monoclinic tridymite.

Triclinic $AlPO_4$

Crystal data

$AlPO_4$
M_r = 121.95
Triclinic, $F1$
a = 10.0132 (4) Å
b = 17.3635 (6) Å
c = 82.496 (3) Å
α = 90.006 (8)°
β = 90.026 (4)°
γ = 89.983 (5)°
V = 14343.2 (9) Å^3
Z = 160
D_x = 2.259 (1) Mg m^{-3}
Cu $K\alpha_1$ radiation
Cell parameters from 5601 reflections
θ = 5–45°
μ = 8.161 mm^{-1}
T = 295 K
Specimen shape: cylinder (0.5 mm capillary)
Specimen prepared at 1273 K
Particle morphology: plate-like
White powder

Data collection

Siemens D5000 diffractometer
θ–2θ scans
Specimen mounting: 0.5 mm glass capillary
Specimen mounted in transmission mode
5601 measured reflections
θ_{max} = 45°
$h = 0 \rightarrow 10$
$k = -16 \rightarrow 16$
$l = -76 \rightarrow 76$
$2\theta_{min}$ = 10, $2\theta_{max}$ = 90°
Increment in 2θ = 0.008°

Refinement

Refinement on I_{net}
R_B = 0.033
R_p = 0.016
R_{wp} = 0.022
R_{exp} = 0.012
S = 2.16
$2\theta_{min}$ = 10, $2\theta_{max}$ = 90°
Increment in 2θ = 0.008°
Wavelength of incident radiation: 1.5406 Å
Excluded region(s): none
Profile function: pseudo-Voigt
745 parameters
$w = 1/[Y(\text{obs})]^{1/2}$
$(\Delta/\sigma)_{max}$ = 0.01
$\Delta\rho_{max}$ = 0.39 e Å^{-3}
$\Delta\rho_{min}$ = −0.42 e Å^{-3}
Preferred orientation correction: none

Monoclinic $AlPO_4$

Crystal data

$AlPO_4$
M_r = 121.95
Monoclinic, Pc
a = 37.3863 (16) Å
b = 5.0455 (2) Å
c = 26.2217 (10) Å
β = 117.8164 (13)°
V = 4374.7 (4) Å^3
Z = 48
D_x = 2.222 (1) Mg m^{-3}
Cu $K\alpha_1$ radiation
Cell parameters from 3075 reflections
θ = 7.5–42.5°
μ = 8.027 mm^{-1}
T = 295 K
Specimen shape: cylinder (<0.5 mm capillary)
Specimen prepared at 1223 K
Particle morphology: plate-like
White powder

Data collection

Siemens D5000 diffractometer
θ–2θ scans
Specimen mounting: 0.5 mm glass capillary
Specimen mounted in transmission mode
3075 measured reflections
θ_{max} = 42.5°
$h = 0 \rightarrow 33$
$k = 0 \rightarrow 5$
$l = -23 \rightarrow 23$
$2\theta_{min}$ = 15, $2\theta_{max}$ = 85°
Increment in 2θ = 0.008°

Refinement

Refinement on I_{net}
R_B = 0.073
R_p = 0.017
R_{wp} = 0.023
R_{exp} = 0.015
S = 1.79
$2\theta_{min}$ = 15, $2\theta_{max}$ = 85°
Increment in 2θ = 0.008°
Wavelength of incident radiation: 1.5406 Å
Excluded region(s): none
Profile function: pseudo-Voigt
459 parameters
$w = 1/[Y(\text{obs})]^{1/2}$
$(\Delta/\sigma)_{max}$ = 0.01
$\Delta\rho_{max}$ = 0.89 e Å^{-3}
$\Delta\rho_{min}$ = −0.78 e Å^{-3}
Preferred orientation correction: none

Both crystal structures were refined according to the Rietveld method (Rietveld, 1969) starting with the atomic coordinates of the isotypic silica tridymite phases (monoclinic: Kato & Nukui, 1976; triclinic: Konnert & Appleman, 1978). Lattice parameters, individual scale factors for the three phases and five common peak-shape parameters of the pseudo-Voigt function (No. 2), one asymmetry parameter and one parameter for the zero-point correction were used to describe the powder patterns. The high background at low 2θ caused by the position-sensitive detector was removed by the fixed background subtraction feature of the *GSAS* program package (Larson & von Dreele, 1994) and the remainder was fitted with six parameters using a power series function (No. 6).

Soft constraints were applied to the interatomic distances so that the sizes of the tetrahedra remained close to the average values of $AlPO_4$ quartz: Al—O = 1.733 (1), O—O = 2.833 (2), P—O = 1.523 (1), O—O = 2.488 (2) and Al—P = 3.112 (5) Å (Muraoka & Kihara, 1997). Monoclinic $AlPO_4$ tridymite (space group *Pc*) contains 144 atoms and triclinic tridymite (space group *F*1) 240 atoms in the asymmetric unit. The *x* and *z*, and the *x*, *y* and *z* positional parameters of the first Al atom (Al1) were fixed in order to define the origin in the space groups *Pc* and *F*1, respectively. In the final stages of the refinements, all profile, scale, background, lattice and positional parameters of the main constituent phase were varied simultaneously together with a single overall displacement parameter. Corrections for absorption and extinction were found to be unnecessary. Preferred orientation was not observed. Apart from the zero-point correction, no account has been taken of systematic effects on the lattice parameters.

For both compounds, data collection: *DIFFRAC–AT* (Version 3.0; Siemens, unpublished); cell refinement: *GSAS* (Larson & von Dreele, 1994); data reduction: *GSAS*; program(s) used to solve structure: *GSAS*; program(s) used to refine structure: *GSAS*; molecular graphics: *WATOMS* (Dowty, 1994); software used to prepare material for publication: *WINWORD* (Version 6.0).

The work was partly supported by the Deutsche Forschungsgemeinschaft.

Supplementary data for this paper are available from the IUCr electronic archives (Reference: BR1269). Services for accessing these data are described at the back of the journal.

References

Baur, W. H. (1977). *Acta Cryst.* B**33**, 2615–2619.
Dowty, E. (1994). *WATOMS*. Version 3.0. Shape Software, 521 Hidden Valley Road, Kingsport, TN 37663, USA.
Kato, K. & Nukui, A. (1976). *Acta Cryst.* B**32**, 2486–2491.
Kihara, K. (1995). *Phys. Chem. Miner.* **22**, 223–232.
Konnert, J. & Appleman, D. (1978). *Acta Cryst.* B**34**, 391–401.
Larson, A. C. & von Dreele, R. B. (1994). *LANSCE* (MS-H805). Report LAUR 86–748. Los Alamos National Laboratory, Los Alamos, New Mexico, USA.
Löns, J., Mann, K. & Hoffmann, W. (1989). *Eur. J. Mineral.* **1**, 113.
Muraoka, Y. & Kihara, K. (1997). *Phys. Chem. Miner.* **24**, 243–253.
Pryde, A. K. A. & Dove, M. T. (1998). *Phys. Chem. Miner.* **26**, 171–179.
Rietveld, H. M. (1969). *J. Appl. Cryst.* **2**, 65–71.
Spiegel, M., Hoffmann, W. & Löns, J. (1990). *Eur. J. Mineral.* **2**, 246.